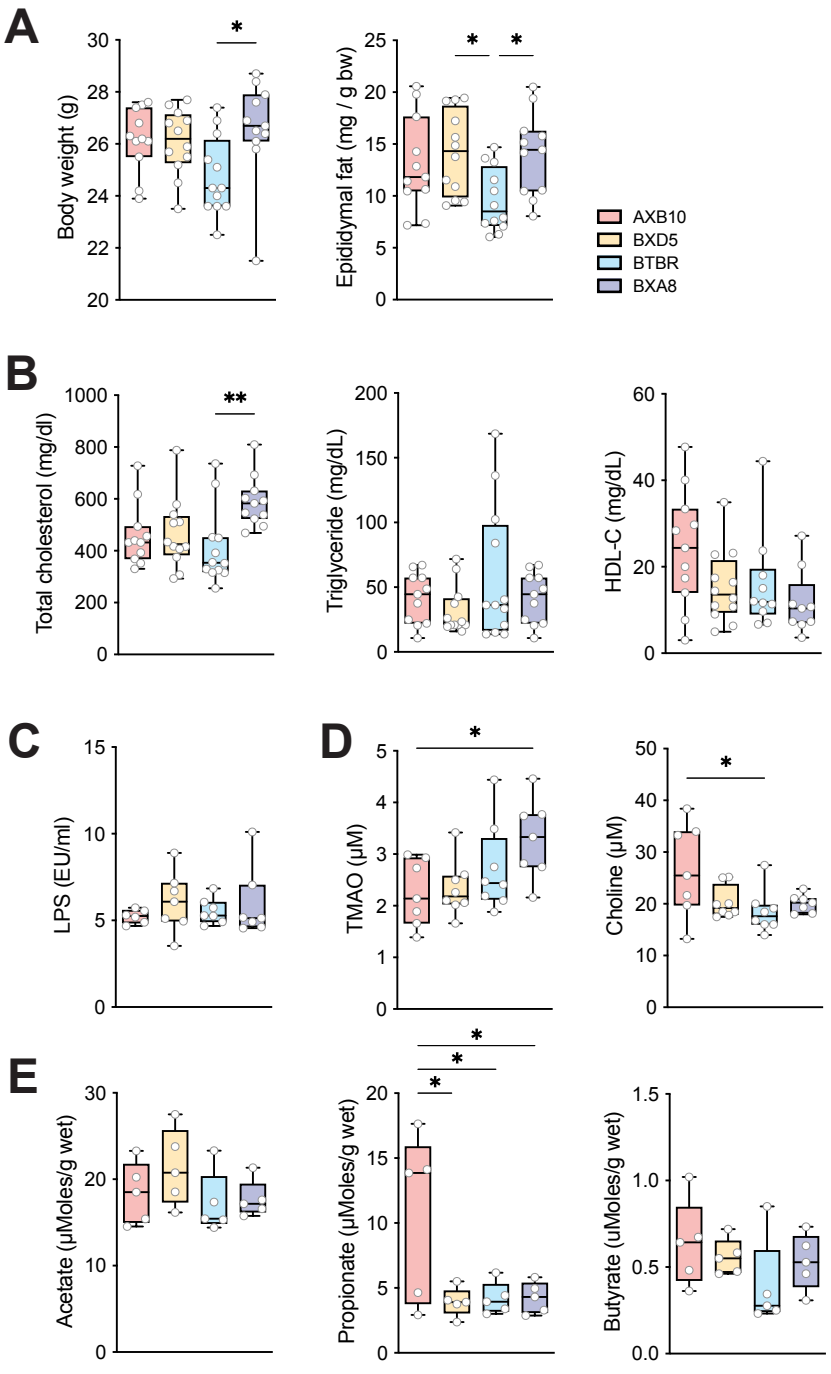

Supplementary Figure 1. Body weight, lipid profile, and microbial metabolites from transplanted mice, related to Figure 1. A) Body weight and epididymal fat weight collected at the end of the experiment. B) Total cholesterol, triglyceride, and HDL-cholesterol in plasma. C) Plasma lipopolysaccharide (LPS) levels. D) Plasma TMAO and choline levels. E) Cecal acetate, propionate, and butyrate levels. Data are shown as box-and-whisker plots with individual data points, where the boxes indicate the median values and the interquartile ranges and the whiskers represent the minimum and maximum values. Significance was calculated by one-way ANOVA with the Tukey post-tests and is reported as follows: *, p-value of <0.05; **, p-value of <0.01.

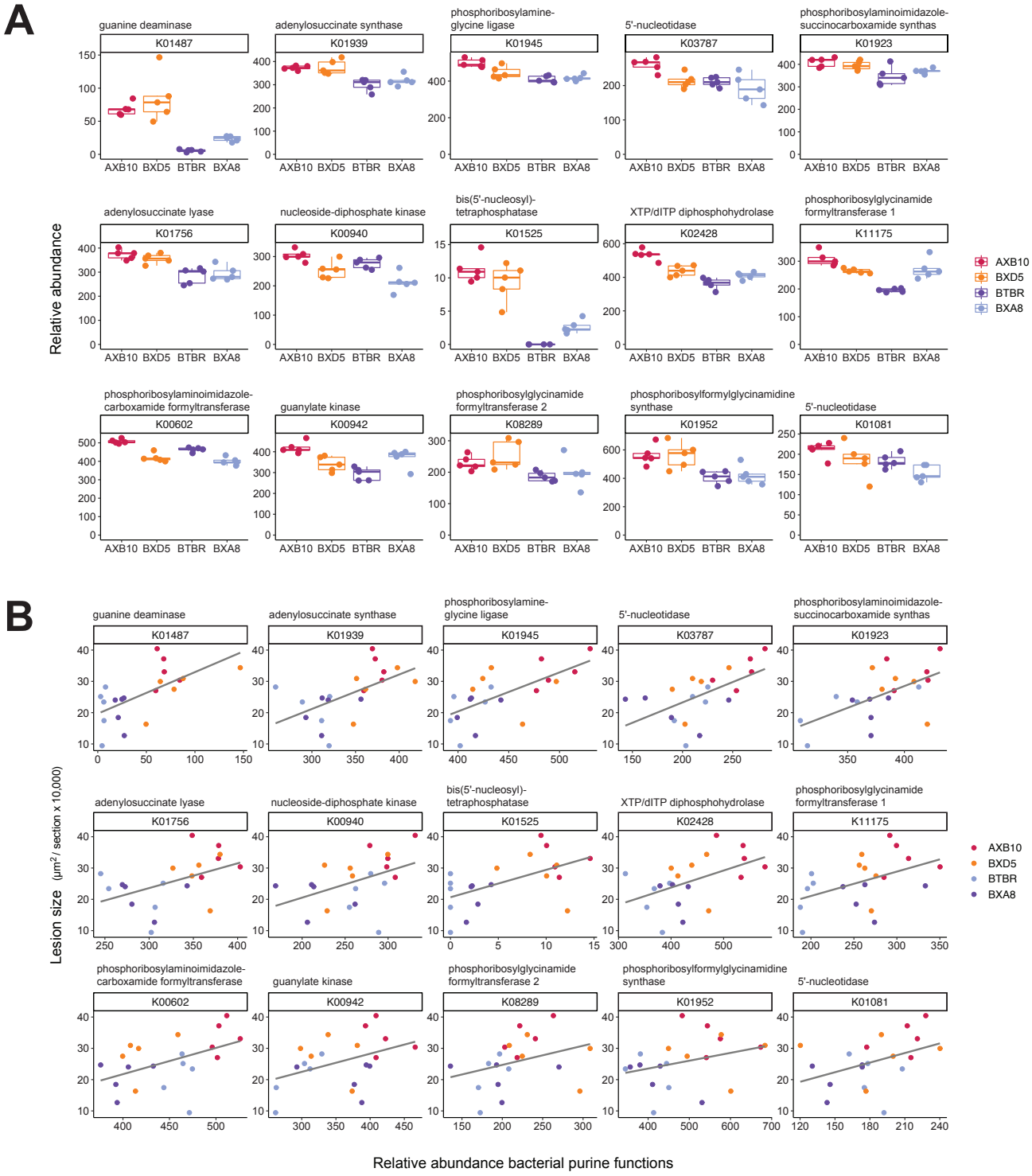

Supplementary Figure 2. Metagenomic analysis of transplanted *ApoE* knockout mice, related to Figure 1. A) Relative abundance of molecular functions (Kegg Orthology, KO) involved in purine metabolism in transplanted *ApoE* knockout mice. B) Spearman correlation between bacterial KO involved in purine and atherosclerosis lesion size.

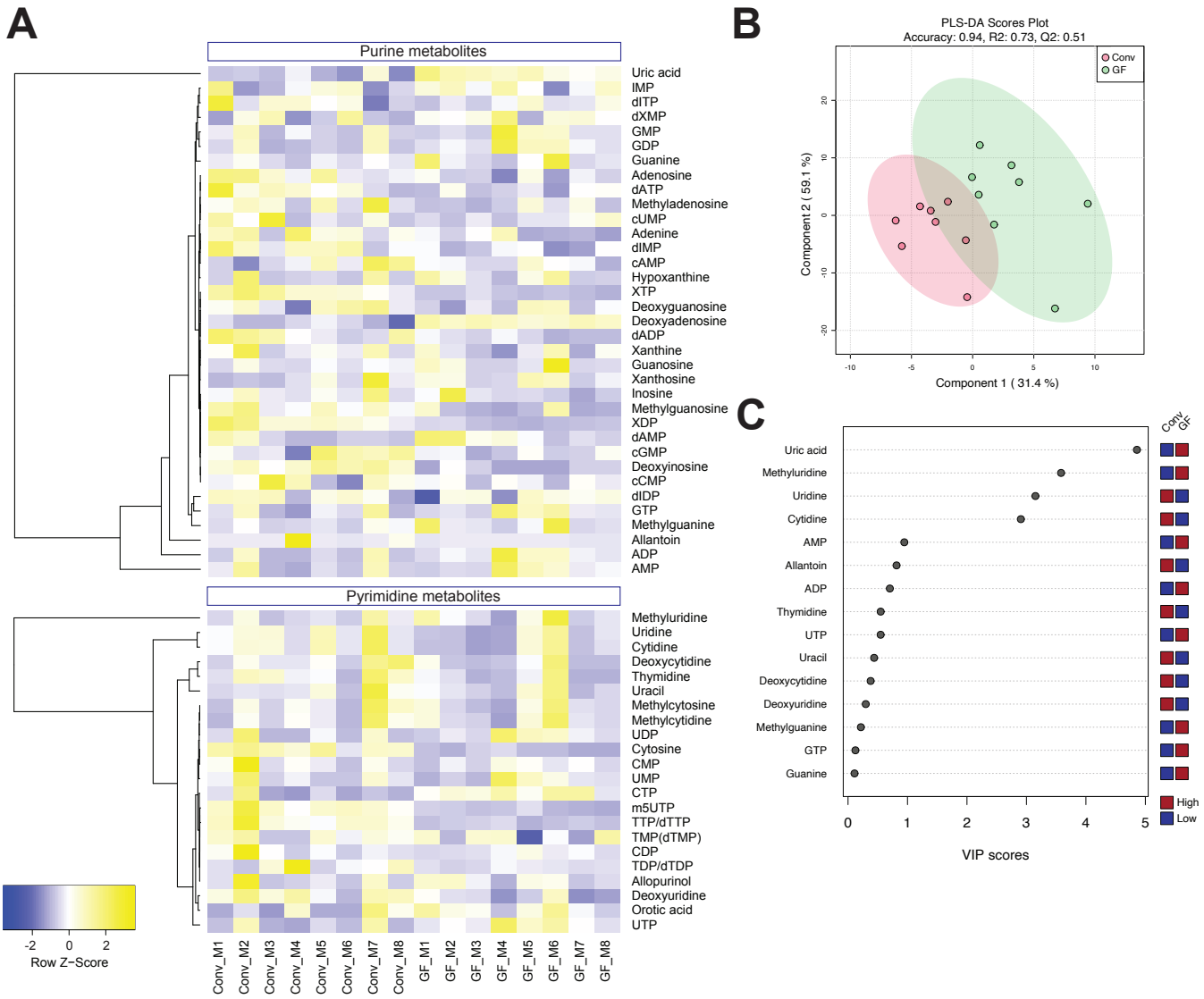

Supplementary Figure 3. Targeted purine metabolite quantitation in plasma samples from Conv and GF mice, related to Figure 3. A) Heatmap of purines and related metabolites in plasma samples from Conv (n=8) and GF (n=8) mice analyzed by LC-MS/MS. B) PLS-DA plot based on the data derived from purine metabolites in plasma samples from Conv and GF mice. C) VIP plot indicating the most discriminating metabolites in descending order of importance. The colored boxes on the right indicate the relative concentrations of the corresponding metabolite in each group. Conv; Conventionally-raised, GF; germ-free, PLS-DA; Partial Least Squares Discriminant Analysis, VIP; variable importance of projection.

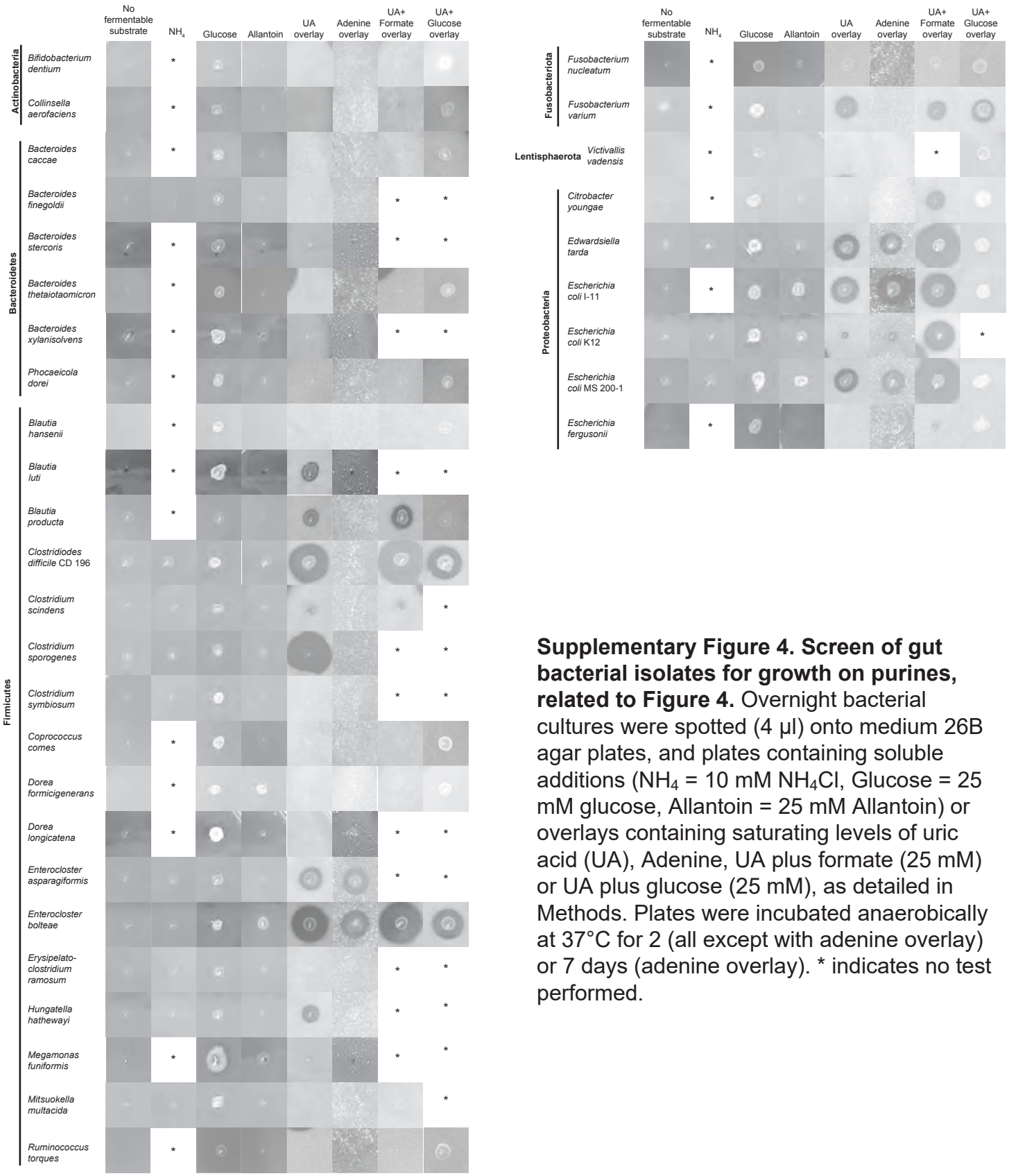

Supplementary Figure 4. Screen of gut bacterial isolates for growth on purines, related to Figure 4. Overnight bacterial cultures were spotted (4 µl) onto medium 26B agar plates, and plates containing soluble additions (NH_4 = 10 mM NH_4Cl, Glucose = 25 mM glucose, Allantoin = 25 mM Allantoin) or overlays containing saturating levels of uric acid (UA), Adenine, UA plus formate (25 mM) or UA plus glucose (25 mM), as detailed in Methods. Plates were incubated anaerobically at 37°C for 2 (all except with adenine overlay) or 7 days (adenine overlay). * indicates no test performed.

A

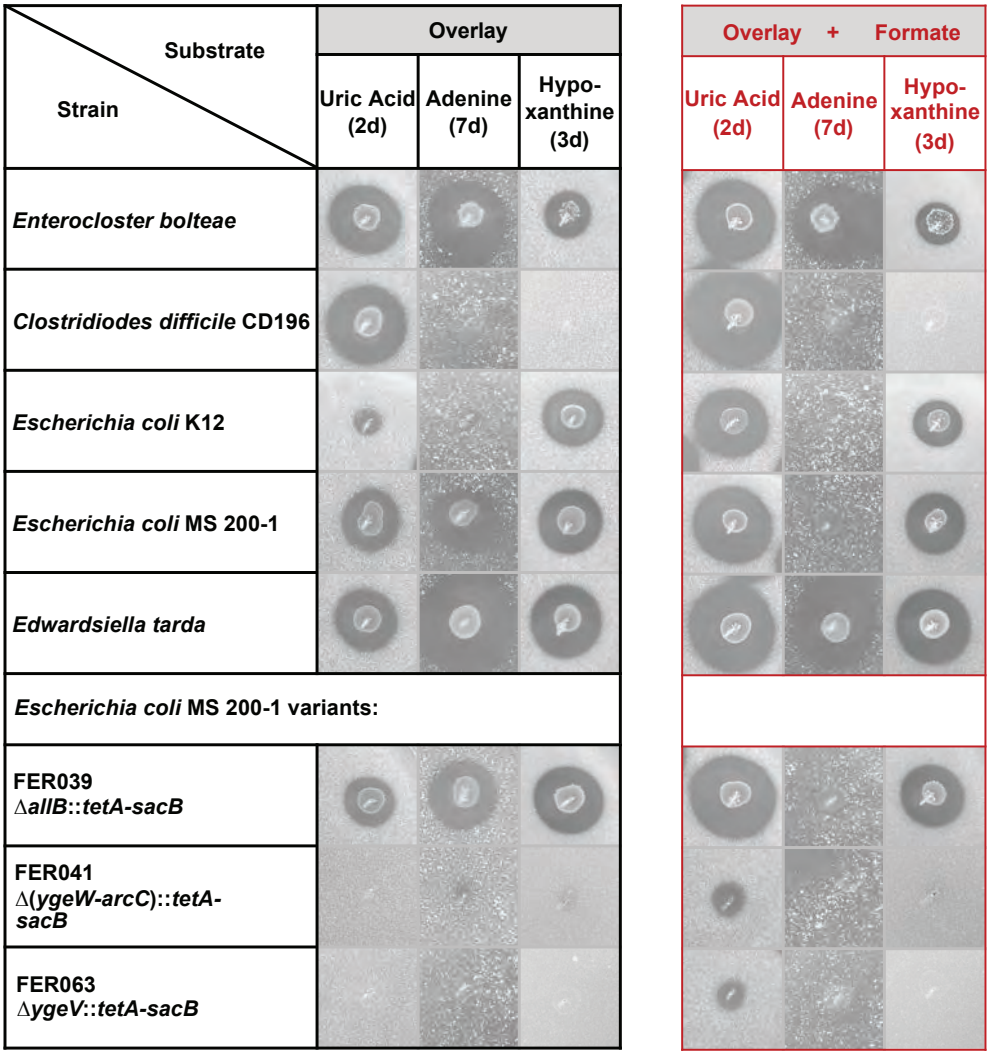
Substrate
Strain
Overlay
Uric Acid (2d)
Adenine (7d)
Hypo-xanthine (3d)
Overlay + Formate
Uric Acid (2d)
Adenine (7d)
Hypo-xanthine (3d)
Enterocloster bolteae
Clostridiodes difficile CD196
Escherichia coli K12
Escherichia coli MS 200-1
Edwardsiella tarda
Escherichia coli MS 200-1 variants:
FER039 ΔallB::tetA-sacB
FER041 Δ(ygeW-arcC)::tetA-sacB
FER063 ΔygeV::tetA-sacB

B

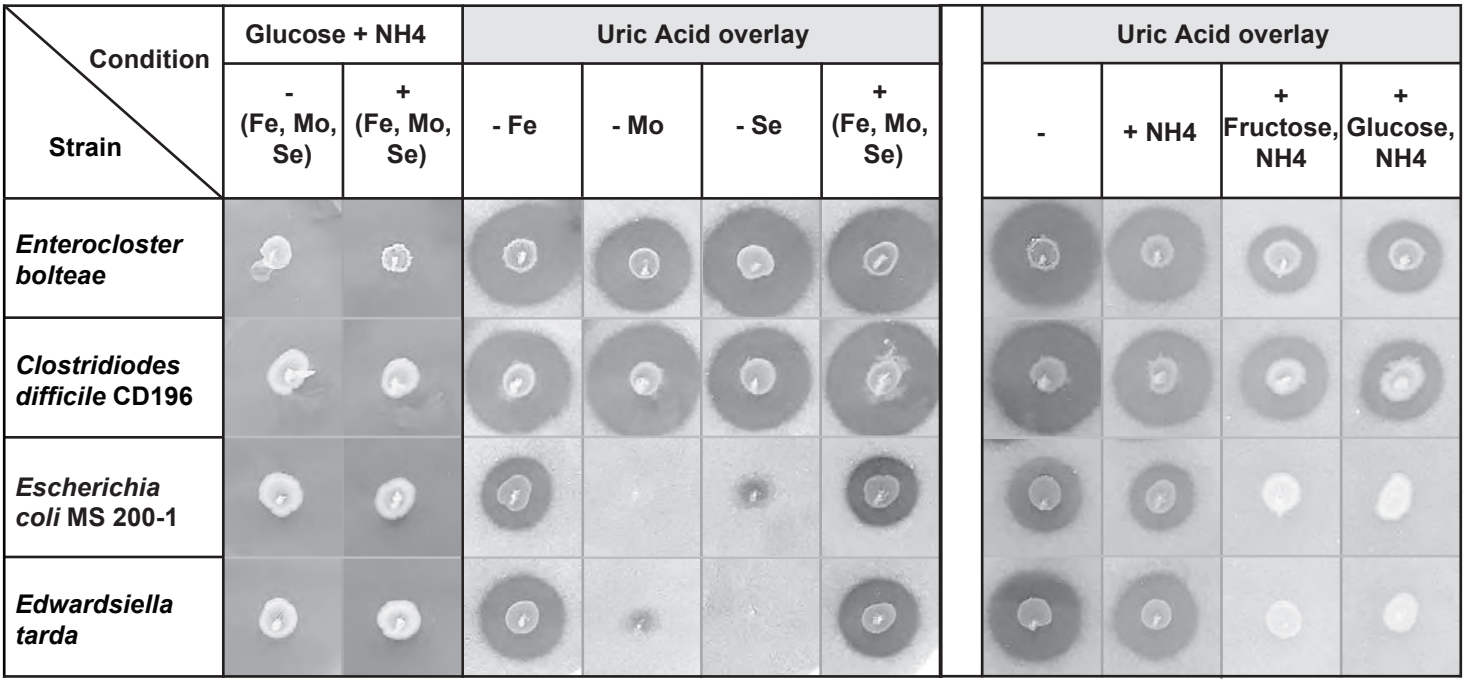
Condition
Strain
Glucose + NH4
- (Fe, Mo, Se)
+ (Fe, Mo, Se)
Uric Acid overlay
- Fe
- Mo
- Se
+ (Fe, Mo, Se)
Uric Acid overlay
-
+ NH4
+ Fructose, NH4
+ Glucose, NH4
Enterocloster bolteae
Clostridiodes difficile CD196
Escherichia coli MS 200-1
Edwardsiella tarda

Supplementary Figure 5. Enviromental factors influence purine utilization, related to Figure 4. A) Formate. Several Firmicutes and Proteobacteria species were spotted onto purine (Uric Acid, Adenine, Hypoxanthine) overlay plates and otherwise identical media supplemented with filter-sterilized formate (pH 7, 25 mM in both the base and overlay layers). As previously reported for cell suspensions of *Escherichia coli* K12, UA utilization was enhanced in the presence of formate. Similar results are evident for *E. coli* MS 200-1 and the purine-utilizing allB variant (FER039) as well as for *Edwardsiela tarda*. The enhanced UA utilization is less pronounced with the two tested Firmicutes (*Enterocloster bolteae* and *Clostridiodes difficile*), and is not evident for any strain for adenine and hypoxanthine, which are more reduced than UA. The slight utilization of UA in the presence of formate by the variants FER041 and FER063 suggests the presence of a second, perhaps adventitious, UA-utilization system. B) Trace minerals and sugars. Trace minerals: Plates containing 20 mM glucose + 10 mM NH_4Cl, or bilayer uric acid overlay plates were prepared with different trace mineral compositions: i) containing all trace element additions (see Methods with 2.5 µM Fe, 5 µM Mo and 0.5 µM Se) or ii) lacking the addition of the indicated trace element. No attempt was made to rigorously remove the “missing” minerals, and plates were prepared with otherwise standard cysteine·HCl-reduced, phosphate-buffered medium 26B containing 0.1% yeast extract and Difco Bacto agar. Sugars: Standard bilayer uric acid plates were prepared (see Methods) or supplemented with filter-sterilized stocks of NH_4Cl (to 10 mM), fructose and NH_4Cl (to 40 and 10 mM, respectively), or glucose + NH_4Cl (to 40 and 10 mM, respectively). Plates were spotted with 4 µl of cultures freshly-grown in rich medium and incubated anaerobically for 2 days at 37°C.

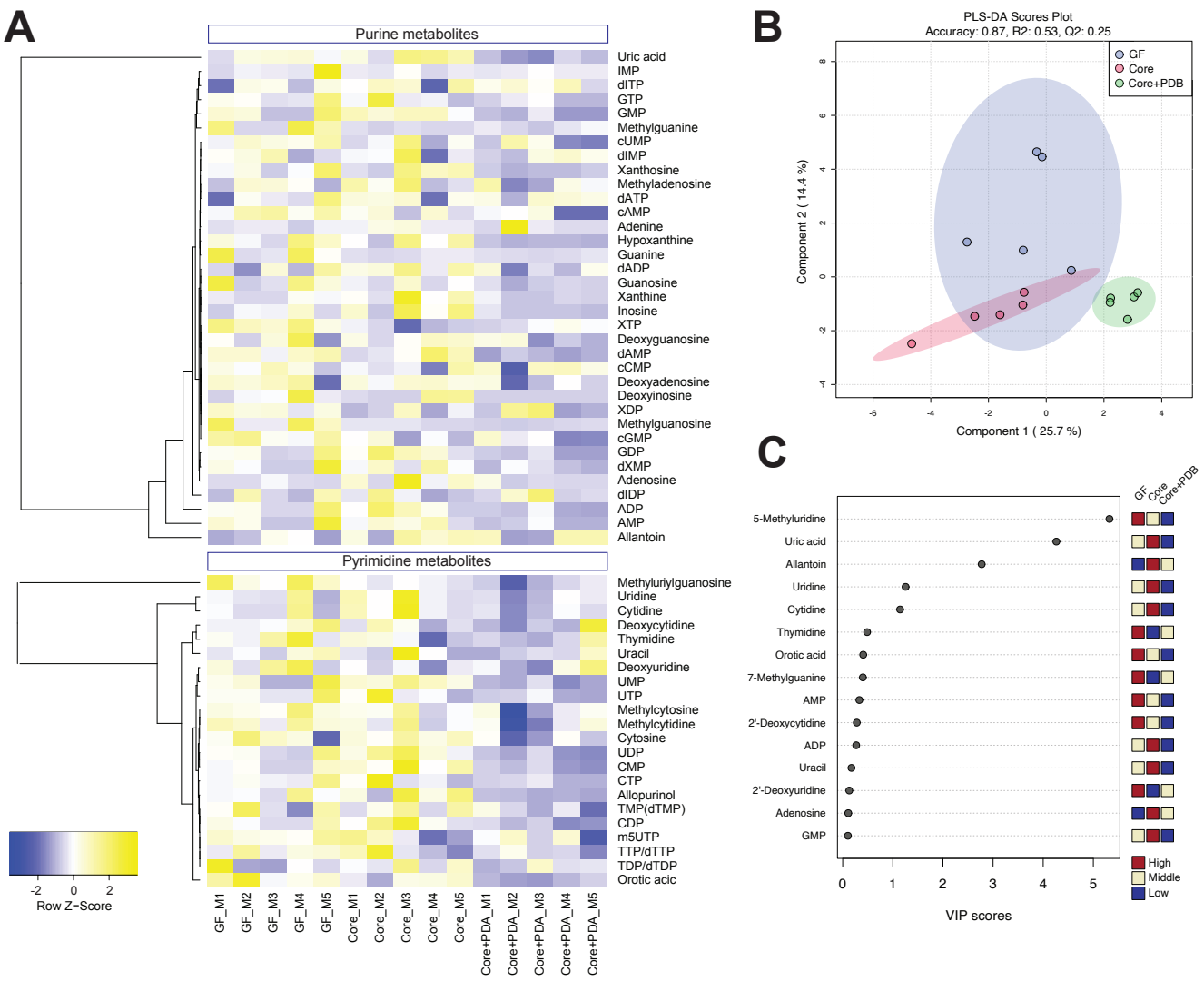

Supplementary Figure 6. Targeted purine metabolite quantitation in plasma samples from GF and gnotobiotic mice, related to Figure 5. A) Heatmap of purines and related metabolites in plasma samples from GF (n=5), 'core' (n=3) and 'core plus PDB' (n=5) mice analyzed by LC-MS/MS. B) PLS-DA plot based on the data derived from purine metabolites in plasma samples from GF, 'core' and 'core plus PDB' mice. C) Variable Importance Projection plot indicating the most discriminating metabolites in descending order of importance. The colored boxes on the right indicate the relative concentrations of the corresponding metabolite in each group. GF; germ-free, PDB; purine-degrading bacteria, PLS-DA; Partial Least Squares Discriminant Analysis, VIP; variable importance of projection.

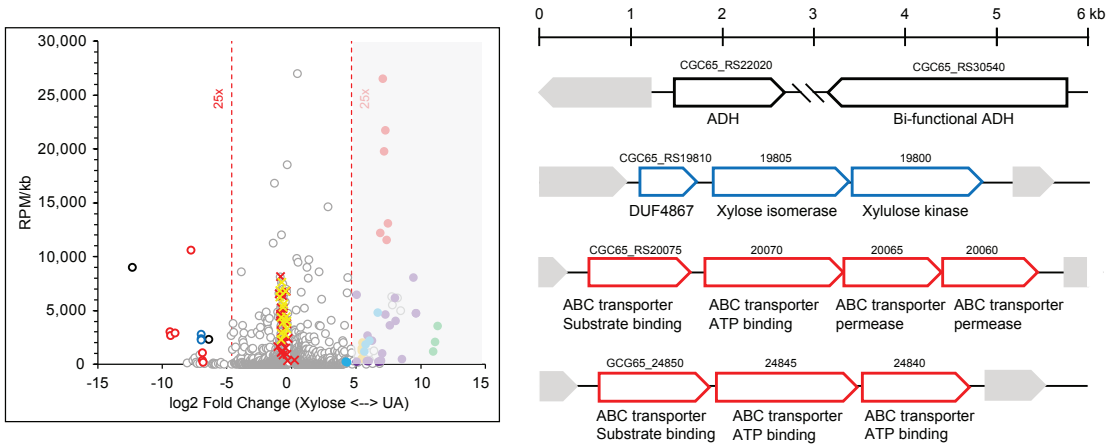
RPM/kb
log2 Fold Change (Xylose <--> UA)
25x
25x
0 1 2 3 4 5 6 kb
CGC65_RS22020
CGC65_RS30540
ADH
Bi-functional ADH
CGC65_RS19810
19805
19800
DUF4867
Xylose isomerase
Xylulose kinase
CGC65_RS20075
20070
20065
20060
ABC transporter Substrate binding
ABC transporter ATP binding
ABC transporter permease
ABC transporter permease
GCG65_24850
24845
24840
ABC transporter Substrate binding
ABC transporter ATP binding
ABC transporter ATP binding

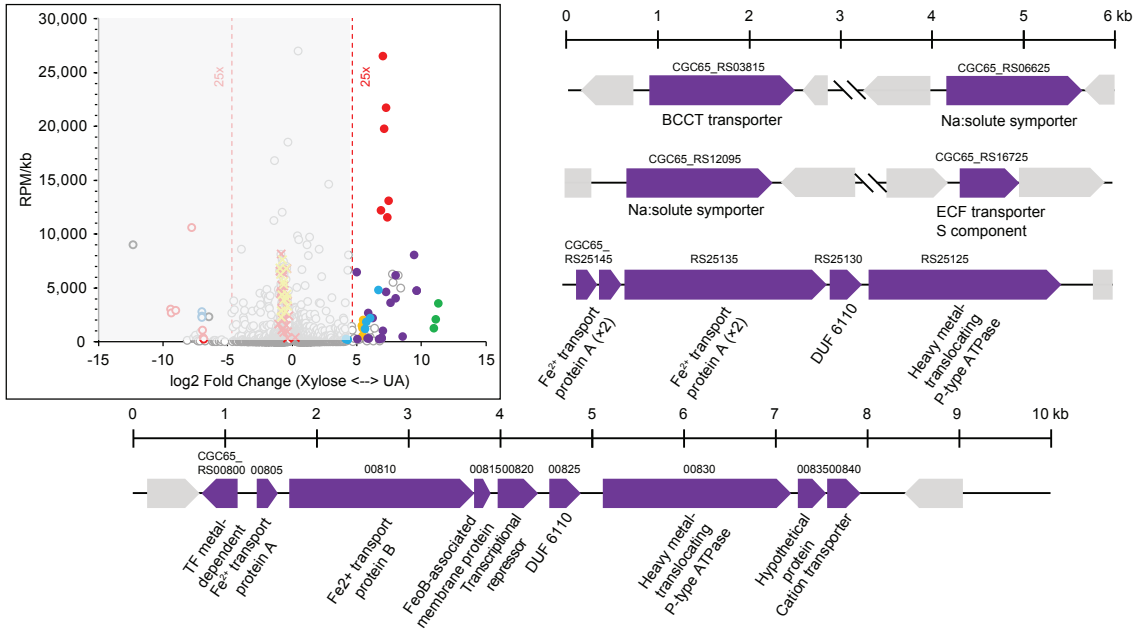
RPM/kb
log2 Fold Change (Xylose <--> UA)
25x
25x
0 1 2 3 4 5 6 kb
CGC65_RS03815
CGC65_RS06625
BCCT transporter
Na:solute symporter
CGC65_RS12095
CGC65_RS16725
Na:solute symporter
ECF transporter S component
CGC65_ RS25145
RS25135
RS25130
RS25125
Fe2+ transport protein A (x2)
Fe2+ transport protein A (x2)
DUF 6110
Heavy metal-translocating P-type ATPase
0 1 2 3 4 5 6 7 8 9 10 kb
CGC65_ RS00800
00805
00810
0081500820
00825
00830
0083500840
TF metal-dependent Fe2+ transport protein A
Fe2+ transport protein B
FeoB-associated membrane protein
Transcriptional repressor
DUF 6110
Heavy metal-translocating P-type ATPase
Hypothetical protein
Cation transporter

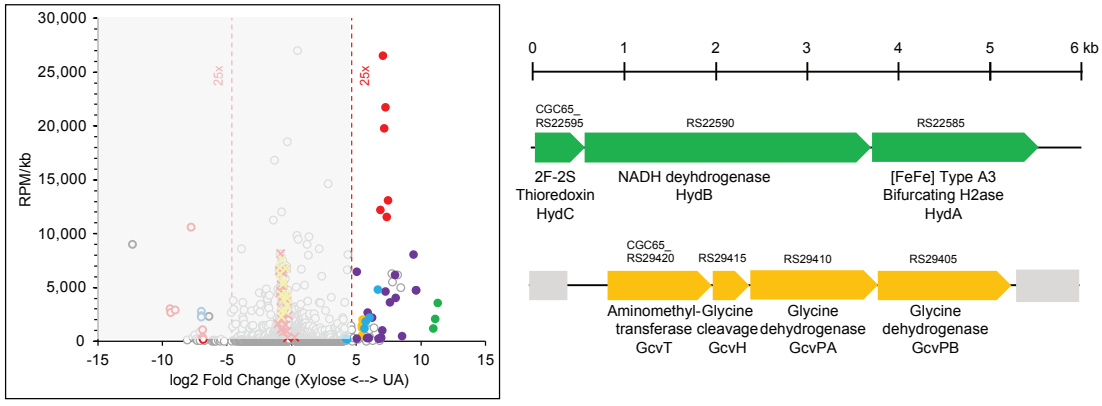
RPM/kb
log2 Fold Change (Xylose <--> UA)
25x
25x
0 1 2 3 4 5 6 kb
CGC65_ RS22595
RS22590
RS22585
2F-2S Thioredoxin HydC
NADH deyhdrogenase HydB
[FeFe] Type A3 Bifurcating H2ase HydA
CGC65_ RS29420
RS29415
RS29410
RS29405
Aminomethyl-transferase GcvT
Glycine cleavage GcvH
Glycine dehydrogenase GcvPA
Glycine dehydrogenase GcvPB

Supplementary Figure 7. Comparison of transcriptional profiles for *Enterocloster bolteae* grown on xylose vs. uric acid, related to Figure 6. Plot showing differentially-expressed genes (FDR <0.01) and reads per million (RPM)/ gene size (kb) for *Enterocloster bolteae* grown on xylose + NH_4Cl (upregulated genes to the left) or uric acid (upregulated genes to the right). Genes encoding 30S and 50S RNA Polymerase (RNAP) subunits are indicated near the center of the figure (yellow and red “x” symbols, respectively) with a slight bias (1.6-fold) towards the xylose substrate side (left) in good agreement with the faster growth rate observed on this substrate and growth rate-limiting nature of RNAP subunit expression. Growth on xylose + NH_4Cl elicited high expression of genes for sugar transport functions, an operon encoding xylose-utilization proteins, and alcohol dehydrogenases, the latter in consistent with the accumulation of ethanol in these cultures (not shown). In addition to the two operons described in the manuscript, growth on uric acid also induced high expression of micronutrient transport functions, one of three glycine cleavage systems, and a bifurcating hydrogenase system. Relevant genes are indicated in the right-hand panels, color-coded according to the expression plots shown on the left.